The initial growth of PTCDA on Cu(111) studied by STM

2007 J. Phys.: Condens. Matter 19 056009

(http://iopscience.iop.org/0953-8984/19/5/056009)

INSTITUTE OF PHYSICS PUBLISHING JOURNAL OF PHYSICS: CONDENSED MATTER

J. Phys.: Condens. Matter **19** (2007) 056009 (12pp) doi:10.1088/0953-8984/19/5/056009

The initial growth of PTCDA on Cu(111) studied by STM

Th Wagner, A Bannani, C Bobisch, H Karacuban and R Möller

Universität Duisburg-Essen, Lotharstraße 1-21, 47057 Duisburg, Germany

E-mail: thorsten.wagner@uni-due.de

Received 7 October 2006, in final form 11 December 2006
Published 15 January 2007
Online at stacks.iop.org/JPhysCM/19/056009

Abstract

The initial growth of 3,4,9,10-perylene-tetracarboxylic-dianhydride (PTCDA) was analysed. Ultrathin films with coverages of up to two layers were prepared on a (111) orientated copper single crystal by means of vapour deposition in an ultrahigh-vacuum chamber. The films were characterized *in situ* by scanning tunnelling microscopy (STM). Within the first layer, two different structures were found. Both exhibit a herringbone-like arrangement of the molecules, which is also found in the (102) plane of the α and β bulk phases. The two-dimensional unit cell is given by two molecules which are rotated by about 90°. As an effect of the interaction with the substrate, a voltage-dependent moiré pattern was observed for one of these phases. For the second layer, a herringbone phase was found that is denser than the phases of the first layer but less dense than the bulk phases.

(Some figures in this article are in colour only in the electronic version)

1. Introduction

Photosensors, solar cells and organic light emitting devices (OLEDs) [1] are applications that have been realized for organic semiconductors. The efficiencies of such devices depend strongly on the quality of the organic adlayers [2]. Due to lattice mismatch and other interactions with the substrate, the first adsorbate layer often differs significantly from the bulk structures. This is especially true for 3,4,9,10 perylene-tetracarboxylic-dianhydride (PTCDA; see figure 1).

The growth of thick layers of PTCDA is the subject of several studies. By means of STM, films with a nominal coverage of up to 20 monolayers were studied on different metallic substrates. Irrespective of the substrate, the formation of small crystallites was found [3, 4]. Chkoda and co-workers [5] found a substrate-temperature-induced transition from layer-by-layer growth to island growth on Ag(111). The experimental data suggest that the first layers of PTCDA on a variety of substrates are stressed.

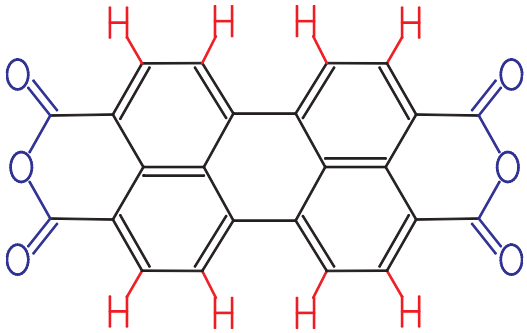

Figure 1. Structure of 3,4,9,10 perylene-tetracarboxylic-dianhydride. The flat molecule has a size of 0.92 nm × 1.42 nm.

A recent study by means of special high-resolution low-energy electron diffraction (LEED), so-called spot profile analysed LEED, confirmed this. Kilian *et al* [6] showed that PTCDA on Ag(111) does not grow in a 'true epitaxial mode', meaning that the misfit between the lattice constants of the substrate and the bulk phase of the organic material is released by different lattices throughout the adsorbate film. Due to the misfit of the lattice, the first two layers are stressed. Therefore we will discuss the interaction of the first two layers of PTCDA with the Cu(111) substrate. Besides the structural changes which are related to stress within the first layers, we will also discuss the effects on the electronic structure of the molecules due to their local adsorption environment.

For over 20 years, PTCDA has been one of the model systems for the adsorption of organic dyes on metallic and semiconducting substrates. Although the growth of PTCDA has been studied intensively on gold and silver single-crystal surfaces (see [7] for a review), there are only a few papers related to growth on copper. Schuerlein and Amstrong determined the structure of PTCDA on Cu(100) using LEED [8]. In our group the initial growth on Cu(110) was studied by means of scanning tunnelling microscopy (STM) [9, 10]. It was shown that the strong interaction between the surface and PTCDA leads to a reconstruction of the copper surface. Such *et al* [11] focused in their recent nc-AFM (non-contact or frequency-modulated atomic force microscopy) study on the topographic differences between the first and second layers of PTCDA on Cu(111). They also found herringbone-like unit cells, but did not present any detailed structural data on these.

2. Experimental setup

The experiments were carried out in a multichamber ultrahigh-vacuum (UHV) system. The system consists of three chambers for preparation (sputtering, heating, organic molecular beam epitaxy), analysis (photoelectron spectroscopy, LEED) and STM. To maintain the cleanliness of the sample, the base pressure in all chambers was below 5×10^{-10} mbar. The substrate was a Cu(111) single crystal, which was cleaned by repeated cycles of argon sputtering ($U = 1.5$ kV, $i = 15\ \mu\text{A cm}^{-2}$ for 15 min) and subsequent annealing ($T = 820$ K for 60 min). X-ray photoelectron spectroscopy and STM measurements were applied to confirm that the sample was clean.

Commercially available PTCDA powder (Sigma-Aldrich) was used as a starting material. Before performing the experiments, the crucible containing the molecule was held slightly below the evaporation temperature for several hours. This procedure was carried out to outgas the impurities which are more volatile than PTCDA.

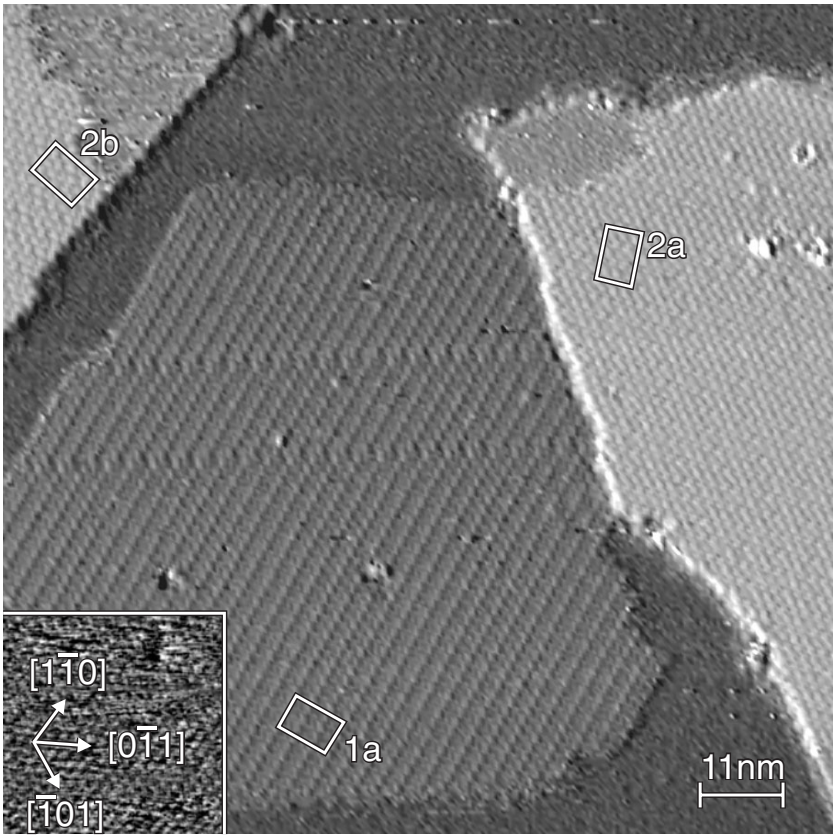

Figure 2. About 0.4 monolayers of PTCDA on Cu(111). The imaged area of the sample is 110 nm × 110 nm. The tunnelling parameters were $U_{\text{bias}} = -0.6$ V and $I_{\text{setpoint}} = 3.9$ pA. The white rectangles symbolize three by three times enlarged unit cells in different domains. The inset shows the same Cu(111) surface with atomic resolution. The image has a size of 4.8 nm × 4.8 nm. To obtain atomic resolution of the Cu(111) surface, the tunnelling parameters were chosen as $U_{\text{bias}} = -0.13$ V and $I_{\text{setpoint}} = 300$ pA.

During the preparation of the films, the sample was held at room temperature. The deposition rate (about $1 \ldots 2$ monolayer min^{-1}) was checked by a quadrupole mass spectrometer (Pfeiffer QMG522). The monitored mass of 392 u corresponds to the intact molecule. The rate was calibrated by thermal desorption spectroscopy (TDS). The signal of the second adsorbate layer arises in the spectra as a separate peak. The area under this peak will not increase any more once saturation has been reached, and it corresponds to the equivalent of one monolayer. In addition, the coverage was checked by large-scale STM scans.

The topographic images were taken with a home-built UHV STM operating at room temperature. For the data acquisition, the open-source software GXSM [12] was used. Careful shielding allows the operation of the STM with tunnelling currents as small as 1 pA. The bias voltage U_{bias} was applied to the tip, which was an electrochemically etched tungsten wire. Furthermore, the tip was prepared by electron bombardment and field emission. The STM data were processed by the software WSxM [13]. Only a line-by-line subtraction or plane subtraction as well as an optimization of the contrast were applied to the data, unless otherwise mentioned. The STM was calibrated by imaging clean GaAs(110), Cu(111), and Au(111).

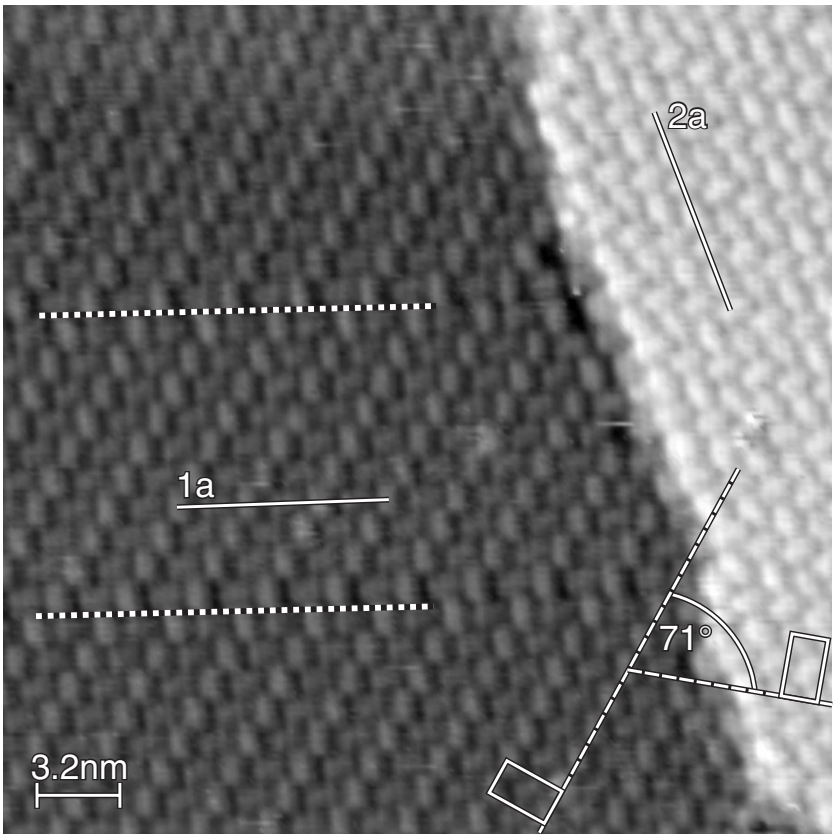

Figure 3. This close-up shows the crossover from '1a' to '2a'. The image size is 32 nm × 32 nm. The tunnelling parameters were $U_{\text{bias}} = -0.9$ V and $I_{\text{setpoint}} = 3.3$ pA. The solid lines indicate cross-sections discussed later. The dashed lines mark the short side of the unit cells. Two defect rows are labelled with points.

3. Results and discussion

3.1. First layer of PTCDA on Cu(111)

In a first series of experiments, samples with a submonolayer coverage of PTCDA on Cu(111) were prepared. Figure 2 shows a typical STM image of such a sample. Even after thermal annealing of the sample with a linear temperature ramp (1 K s^{-1}, final temperature $T = 450$ K), no major change in the topography was observed. PTCDA molecules form islands with typical diameters of 50–100 nm. The height of the islands corresponds to one molecular layer.

The PTCDA islands are compact and exhibit a uniform structure. There are only a few defect rows, as shown in figure 3. In particular, no terraces with two or more domains were found. In figure 3, two domains stick to one step edge of the copper substrate. The domains do not cross the step edge. This is also true in general. On the other hand, there were no 'free' islands—meaning that all islands were attached to copper steps. This indicates that the growth of PTCDA on Cu(111) begins at the substrate step edges.

Within figure 2, three different domains can be distinguished. In this paper, domains with the same structure but different orientation to the substrate will be labelled by the same number, followed by an alphabetic index that refers to the different orientation relative to the substrate.

Table 1. The table compares different experimental (STM) results for the herringbone structure in the first and second layers of PTCDA on Cu(111) with those of the proposed models (MOD) and the (102) planes of the bulk phases.

Layer	1st layer				2nd layer	Bulk	
Phase	'1'		'2'		*Herringbone*	α [14]	β [15]
	STM	MOD	STM	MOD	STM		
a in nm	1.36	1.28	1.36	1.34	1.34	1.20	1.25
Δa in nm	0.07	<0.26	0.07	<0.06	0.07		
b in nm	2.16	2.21	2.16	2.20	2.03	2.00	1.93
Δb in nm	0.11	<0.26	0.11	<0.06	0.10		
$\angle(\vec{a}, \vec{b})$ (deg)	90	90	92	92	90	90	90
$\Delta\angle(\vec{a}, \vec{b})$ (deg)	5		5		5		

Consequently, the domain on the right and the one on the top left of figure 2 are named '2a' and '2b'. The domains only differ by a rotation of 60°, which is caused by the sixfold symmetry of the substrate. Figure 3 also compares the orientation of the short axis of the '1a' domain and that of the '2a' domain. The angle between these two is 71°. We also found that the short axis of the '1' phase is aligned with the substrate. Therefore the short axis of the '2' phase is rotated by an angle of ±11° to the axis of the substrate. If the orientation of the substrate is known, one can easily distinguish between the two structures. Other differences (e.g. the contrast between the molecules, moiré pattern) which will be discussed later, depend on the tunnelling conditions, so that they may not be visible in every STM image. For various STM images like figure 2, which show several domains, only these two structures have been observed.

For both structures, a unit cell is found that contains two molecules at an angle close to 90° with respect to each other. This herringbone-like pattern was also found for the two bulk phases in the (102) plane [14, 15] and for the adsorption of PTCDA on (111) oriented metal surfaces of silver [16] and gold [17, 18]. This structure can be understood by taking the partial charges of PTCDA into account. The dianhydride groups are negatively charged, whereas the hydrogen atoms of the perylene core carry a positive partial charge. The herringbone arrangement maximizes the coulomb interaction by allowing that every dianhydride group faces a perylene core.

The statistical error for the length and the width of the unit cells is only 0.02 nm. However, the calibration error and other systematic errors are estimated to be 5%. Taking these errors into account, the sizes of the two unit cells, marked by '1' and '2', seem to be the same: $|\vec{a}| = 1.36\ \text{nm} \pm 0.07\ \text{nm}$ and $|\vec{b}| = 2.16\ \text{nm} \pm 0.11\ \text{nm}$. For the angle, which is given by $\vec{a}$ and $\vec{b}$, values between 85° and 95° were measured. With these results, rectangular unit cells are possible, but other structures are not excluded. It is important to mention that, due to thermal drift and piezo hysteresis, it was not possible to measure a significant difference in size and geometry of the type '1' and the type '2' structures.

Table 1 lists the experimental results and the data for the (102) plane of the α and β bulk structures. It is obvious that the parameters found for the first layer structures are slightly bigger than the unit cells for the corresponding bulk layers. It is well known that in the (102) plane of the bulk the PTCDA molecules are tilted by a small angle (5° to 10°, according to [15]). Therefore a bigger unit cell for the first layer is plaussible if the molecules are lying flat on the substrate.

Diagram 4 shows two cross-sections taken along the diagonal of the unit cells of the '1a' and '2b' domains in figure 3. This allows us to compare the height of the two differently orientated molecules within the unit cell. The difference in height for the two molecules within

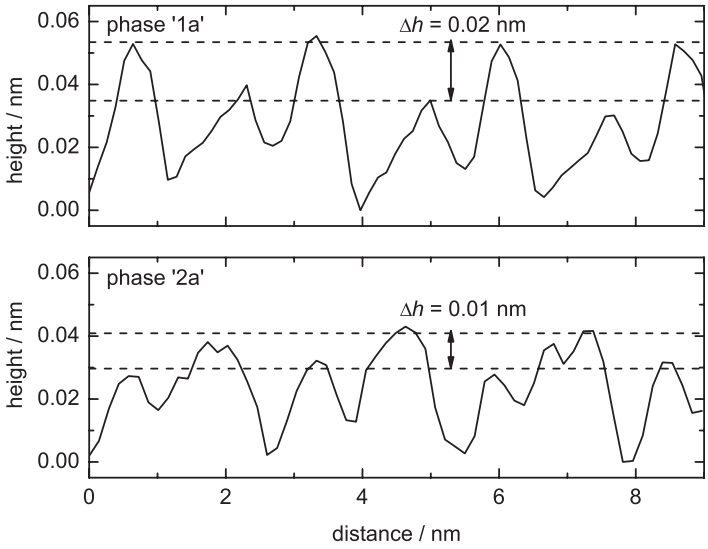

Figure 4. The cross-sections were taken along the diagonals of the '1a' and '2a' unit cells within figure 3.

the '1a' domain is 0.02 nm, whereas is it only 0.01 nm for the '2a' phase. This difference is also visible in the corresponding STM image. For the '1a' phase, the two differently orientated molecules form stripes which show a different height in the STM topography for a certain bias voltage. As the effect for the '2' phases is more than a factor of two smaller, it is not as obvious in the topography. The term 'height' refers here to an 'apparent height', because the topographic images provided by an STM depict a surface of constant local density of states (see [19]).

Figure 5 shows a voltage-dependent contrast of the PTCDA molecules of the '2' phase. With a negatively biased tip, all molecules with the same orientation have the same contrast. As mentioned before, the rows of differently orientated molecules exhibit very small contrast in topography. The molecules themselves appear as longish protrusions which can be attributed to the shape of the molecule (see figure 1). In the consecutive scan (see figure 5(b)) the polarity of the bias voltage was changed. For these parameters the occupied states of the molecules are imaged. The molecules now exhibit a more roundish shape. Additionally, there is a moiré pattern. The stripes can be attributed to a (4×5) supercell. This is an important observation because, for the '1' phase, no such pattern was found. Phase '2' is not a simple superstructure; adjacent molecules (with the same orientation) have different adsorption geometries with respect to the underlying copper lattice. Hoshino *et al* [20] first observed a moiré pattern for PTCDA on HOPG. The authors attributed this effect to a so-called 'point on line' coincidence. The different interactions with the substrate will induce small changes in the electronic structure of the adsorbed molecules, resulting in the observed contrast.

By applying an appropriate voltage to the tip, it was possible to image the PTCDA molecules with submolecular resolution. Figure 6 shows an example. During the scan, the bias voltage was changed. This allows a comparison of the appearance of the molecules at different tip voltages. While there is no structure within the PTCDA at negative voltages, the STM image taken with a positive bias voltage exhibits protrusions which can be related to the internal structure of the PTCDA; where the two hydrogen atoms are bound to the benzene ring there is a small protrusion.

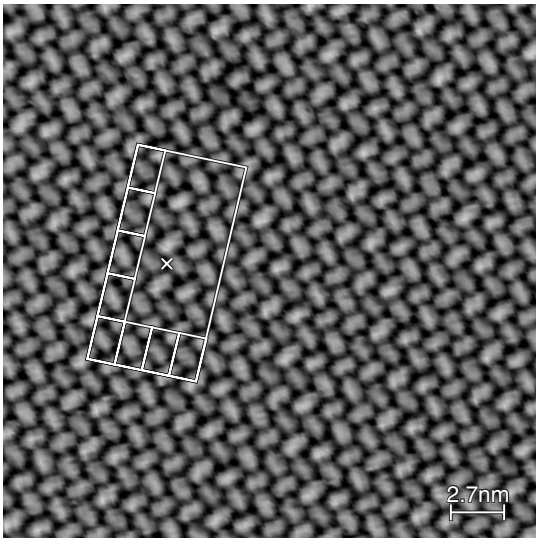

(a) $U_{bias} = -1.1$ V

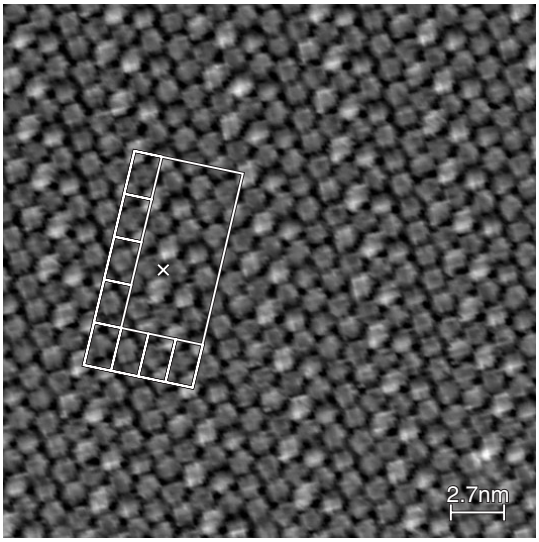

(b) $U_{bias} = +1.1$ V

Figure 5. Voltage-dependent STM images of the '2' phase of PTCDA on Cu(111). The sample had been annealled with a linear temperature ramp ending at 450 K. The images show the same region of the sample, which has a size of 27 nm × 27 nm. The tunnelling current was held constant at $I_{\text{setpoint}} = 4.2$ pA. The image with the positive bias voltage (b) exhibits a moiré pattern, while the one with the negatively biased tip (a) does not.

The experimental results can be explained by the structural models displayed in figure 7. Here figure 7(a) resembles the '1' structure, as marked in figures 2 and 3. The structure can be described by the following matrix equation

$$\begin{pmatrix} \vec{a} \\ \vec{b} \end{pmatrix} = \begin{pmatrix} 0 & 5 \\ 10 & 5 \end{pmatrix} \cdot \begin{pmatrix} \vec{a}_{\text{Cu}} \\ \vec{b}_{\text{Cu}} \end{pmatrix}.$$

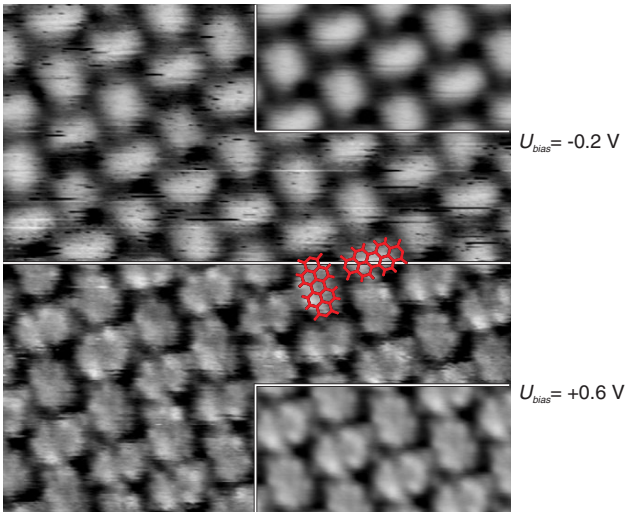

Figure 6. During the acquisition of this STM image, the bias voltage of the tip was changed from −0.2 V (top) to 0.6 V (bottom). The line in the middle of the image marks the scan line when the voltage was changed. To display the upper and the lower part of the image, a step with a height of 0.35 nm (top to bottom) was subtracted. The set-point was about 10 pA. The image size is 10 nm × 10 nm. The two insets were calculated by taking the average over several unit cells within the top and the bottom halves of the image.

Since a simple superstructure is assumed, the matrix elements are integer values. This assumption is based on the experimental observation that no moiré pattern was found for this structure. The orientation of the unit cell was chosen such that the short axis is parallel to a unit cell vector of the underlying substrate. Therefore the (1, 1) element is zero. The proposed unit cell is rectangular, with corresponding vectors of length of $|\vec{a}| = 1.28$ nm and $|\vec{b}| = 2.21$ nm respectively. As the experimental error is smaller than the distance between neighbouring copper atoms of 0.26 nm, one can conclude that the model depicts the experimental data well.

The two molecules within the unit cell are assumed to be rotated by an angle of 90°, which takes the symmetry of the substrate and the molecules into account. Because the two molecules in figure 7(a) do not have the same adsorption site with respect to the lattice of the substrate, it is not surprising that the molecules have a different height in the STM images, as discussed before.

The structures shown in figures 7(b) and (c) are equivalent. They merge if they are mirrored at the marked unit cell vector of the underlying copper lattice. The structure is given by the following matrix equation:

$$\begin{pmatrix} \vec{a} \\ \vec{b} \end{pmatrix} = \begin{pmatrix} 1\frac{1}{4} & 5\frac{3}{4} \\ 9\frac{4}{5} & 3\frac{2}{5} \end{pmatrix} \cdot \begin{pmatrix} \vec{a}_{\mathrm{Cu}} \\ \vec{b}_{\mathrm{Cu}} \end{pmatrix}.$$

As the matrix elements are rational numbers, the '2' structure is not a simple superstructure. The denominators '4' and '5' account for the (4 × 5)-supercell, which is coincident with the copper lattice. Consequently, the matrix elements are exact by $\frac{1}{4}$ and $\frac{1}{5}$, respectively. The proposed unit cell for the '2' structure consists of two vectors with lengths $|\vec{a}| = 1.34$ nm and $|\vec{b}| = 2.20$ nm. The angle between both is 91.9°, so the unit cell is not rectangular. As the uncertainties of the model are comparable to the experimental errors, small deviations of this model are possible.

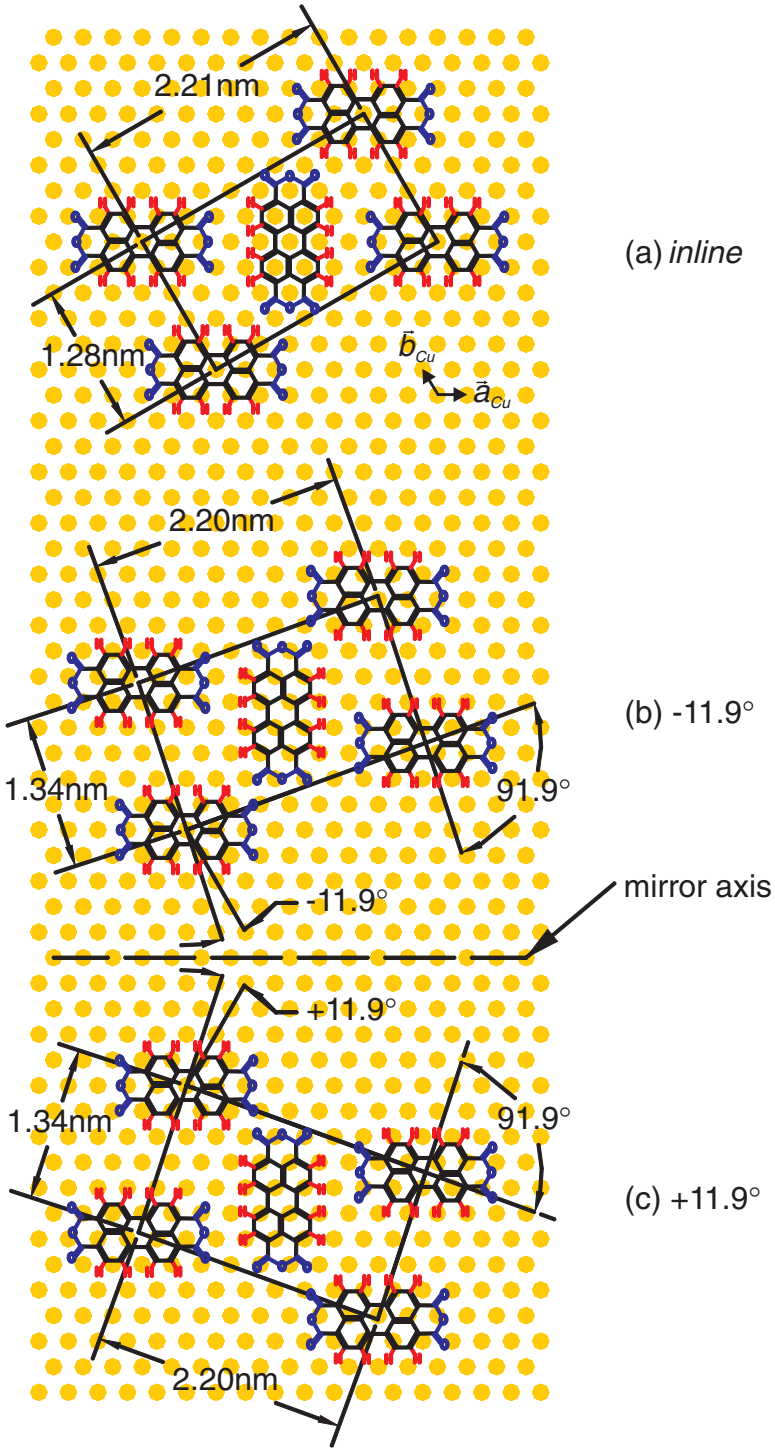

Figure 7. Proposed model of the two structures found for the monolayer of PTCDA on Cu(111): (a) refers to the 'inline' or '1' structure; (b) and (c) refer to structure '2' in two different orientations with respect to the substrate.

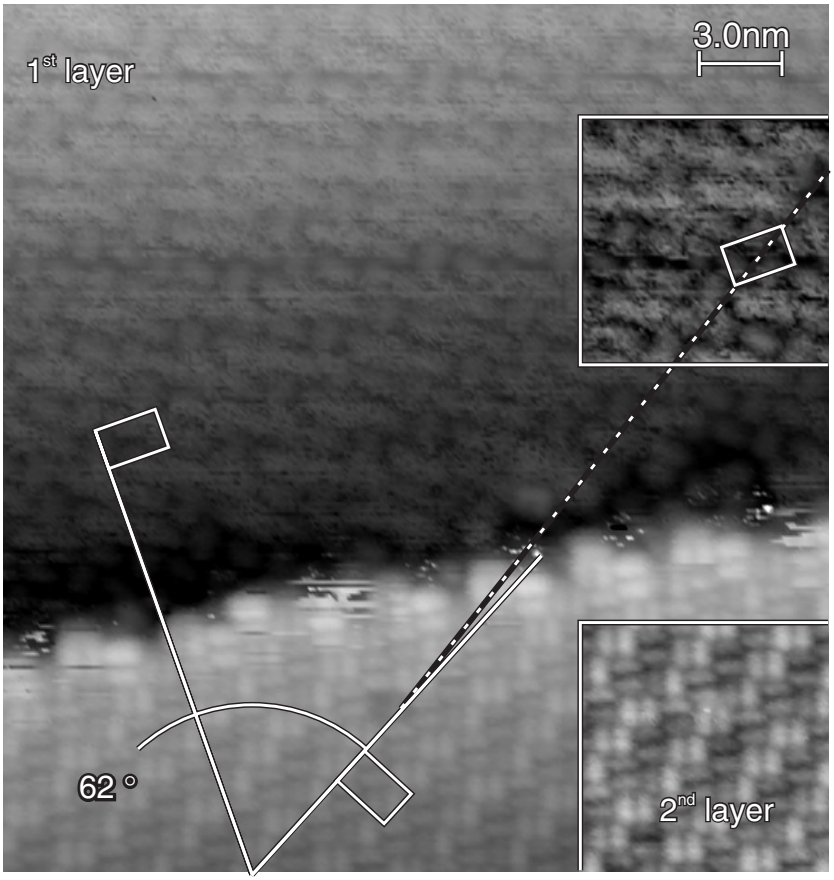

Figure 8. This STM topography shows a Cu(111) surface covered with 1.5 monolayers of PTCDA. The image size is 30 nm × 30 nm. A bias voltage of $U_{\text{bias}} = -2.0$ V was applied to the tip, while the tunnelling current was kept constant at 21 pA. The rectangles mark the unit cells of the first layer (top) and the second layer. The two insets show the structures of the first and second layers, respectively, with optimized contrast.

3.2. Second layer of PTCDA on Cu(111)

The structures for the first layer of PTCDA on Cu(111) are very similar to the (102) planes of the bulk phases, although they are a little bit less dense. The bulk phases mainly differ by a typical shift from one (102) layer to the next. This is also true for nanocrystallites of PTCDA on different metallic surfaces [4]. The experiments in the following section focus on the growth of the second layer, because this layer is important to release the stress between the first layer and the bulk/crystallite phases.

Figure 8 represents a typical image of a Cu(111) surface with more than one monolayer of PTCDA. After the first layer has formed, PTCDA islands grow. The islands of the second layer are also compact. Only the boundaries appear a little bit fuzzy. Submolecular resolution was achieved for the second layer, while in the same image (figure 8) the structure of the first layer was hardly resolved. This indicates that quite a few molecules diffuse on the first layer. The longish shape of the disturbances may indicate that the molecules prefer certain adsorption sites. Additional thermal desorption data—not shown here—support the assumption that the second layer is less bound than the first layer of PTCDA on Cu(111).

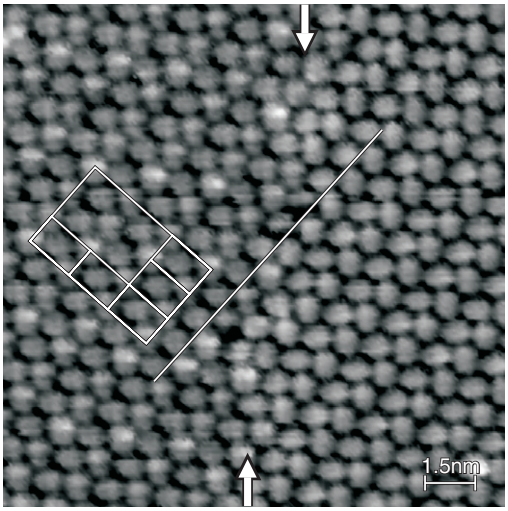

Figure 9. The image shows a 15 nm × 15 nm region with a second layer of PTCDA on Cu(111). The size of the herringbone unit cell is the same within the image, but the internal structure differs on the left and right sides of the two arrows. The image was recorded with $U_{\text{bias}} = +1.6$ V and $I_{\text{setpoint}} = 5$ pA.

Our data on the submolecular structure agree with the findings of Such and co-workers [11]. By means of nc-AFM, they also observed a different appearance of the first and second layers of PTCDA on Cu(111) and attributed this to the different local adsorption environment.

In the second layer, the molecules are arranged in a herringbone-like pattern, as are those in the first layer. The experimental data suggest a rectangular unit cell with $|\vec{a}| = 1.34\ \text{nm} \pm 0.7\ \text{nm}$ and $|\vec{b}| = 2.03\ \text{nm} \pm 0.1\ \text{nm}$. It strikes us that the unit cell of the second layer is a little bit shorter than that of the first layer. One can see from table 1 that the value for the long side of the unit cell is about 5% smaller than the corresponding value of the first layer. Therefore the value for the second layer is closer to the bulk values. The length of the short axis $\vec{a}$ agrees, within the experimental error, with the bulk value. The data in table 1 show that the bulk phase exhibits a denser packing. The density of the herringbone structure of the second layer is between the value of the first layer and the value of the bulk phases. This may indicate that there is a certain stress within the first few layers due to the interaction with the substrate.

The topography presented in figure 8 allows a comparison of the orientation of the unit cell of the first layer to that of the second layer. Based on the assumption that the first layer continues over the whole image, there is not only a shift between the first and second layers but also a rotation. However, this particular image might be misleading due to a possible domain boundary within the first layer which is located at the step edge between the first and second layers. No symmetry line within the first layer can be found to which the unit cell of the second layer aligns. This behaviour is clearly in contrast to the bulk structure, for which only a shift along the short axis (β phase) and the long axis (α phase) of the (102) unit cell was observed. Even for crystallites with a thickness of between 30 and 100 layers, only a simple shift from one layer to the next layer was observed [4].

The formation of the herringbone structure within the second layer seems to be somewhat independent of the underlying layer. The STM topography in figure 9 demonstrates this. The size and the orientation of the herringbone unit cell is the same for the whole image. The

diagonal line indicates this by marking one continuous line of molecules that crosses the image. The two arrows tag a kind of domain boundary where the topography of the molecules on the left and right sides of the line changes. On the right side, the PTCDA seem to form some kind of double row, whereas on the left side they are uniformly spaced. Another striking feature of the left side is that there is a moiré pattern. Its periodicity is given by a (3×3) supercell, which is highlighted by the large rectangle. The small rectangles in figure 9 identify some herringbone unit cells within the supercell.

The observation suggests that the underlying PTCDA layer is not uniform. A domain boundary in the first layer could be the reason for the change in the contrast. The appearance of the moiré pattern and the double line then expresses the different interactions of the first and second layers of PTCDA.

4. Summary and conclusion

In summary, our study of PTCDA on Cu(111) reveals that there are significant interactions not only between the molecules within one layer but also between the molecular layers and the substrate. For the first and second layers of PTCDA on Cu(111), a herringbone-like arrangement of the molecules was found. This arrangement is similar to the (102) plane of the two known bulk phases, although it is less dense. The existence of the herringbone structure, even in ultrathin layers, can be attributed to the strong coulomb interaction between the molecules within one layer.

There is also an interaction between the layers and/or the substrate. The interaction not only modifies the size of the herringbone unit cells but also leads to a modification of the electronic structure of the molecules, as seen by the bias voltage-dependent moiré patterns for the first and second layers. The voltage-dependent contrast of the molecules can be attributed to changes of molecular orbitals due to the interaction with the underlying metallic substrate or organic layer.

References

[1] Sheats J R 1997 *Science* **277** 191–2
[2] Kuzma M 2006 *J. Phys.: Conf. Ser.* **30** 307–20
[3] Stöhr M, Gabriel M and Möller R 2002 *Europhys. Lett.* **59** 423–9
[4] Wagner T, Bannani A, Bobisch C, Karacuban H, Stöhr M, Gabriel M and Möller R 2004 *Org. Electron.* **5** 35–43
[5] Chkoda L, Schneider M, Shklover V, Kilian L, Sokolowski M, Heske C and Umbach E 2003 *Chem. Phys. Lett.* **371** 548–52
[6] Kilian L, Umbach E and Sokolowski M 2004 *Surf. Sci.* **573** 359–78
[7] Barlow S M and Raval R 2003 *Surf. Sci. Rep.* **50** 201–341
[8] Schuerlein T J and Armstrong N R 1994 *J. Vac. Sci. Technol.* A **12** 1992–7
[9] Gabriel M, Stöhr M and Möller R 2002 *Appl. Phys.* A **74** 303–5 http://dx.doi.org/10.1007/s003390101039
[10] Stöhr M, Gabriel M and Möller R 2002 *Surf. Sci.* **507–510** 330–4
[11] Such B, Weiner D, Schirmeisen A and Fuchs H 2006 *Appl. Phys. Lett.* **89** 093104
[12] Zahl P, Bierkandt M, Schroder S and Klust A 2003 *Rev. Sci. Instrum.* **74** 1222–7 webpages of the project: http://gxsm.sf.net and http://sranger.sf.net
[13] WSxM©; http://www.nanotec.es
[14] Lovinger A J, Forrest S R, Kaplan M L, Schmidt P H and Venkatesan T 1984 *J. Appl. Phys.* **55** 476–82
[15] Möbus M, Karl N and Kobayashi T 1992 *J. Cryst. Growth* **116** 495–504
[16] Glöckler K, Seidel C, Soukopp A, Sokolowski M, Umbach E, Bohringer M, Berndt R and Schneider W D 1998 *Surf. Sci.* **405** 1–20
[17] Fenter P, Schreiber F, Zhou L, Eisenberger P and Forrest S R 1997 *Phys. Rev.* B **56** 3046–53
[18] Schmitz-Hübsch T, Fritz T, Sellam F, Staub R and Leo K 1997 *Phys. Rev.* B **55** 7972–6
[19] Tersoff J and Hamann D R 1985 *Phys. Rev.* B **31** 805–13
[20] Hoshino A, Isoda S, Kurata H and Kobayashi T 1994 *J. Appl. Phys.* **76** 4113–20